MOLECULAR PHYSICS, 2003, VOL. 101, NO. 8, 1131–1138

Taylor & Francis
Taylor & Francis Group

Monte Carlo simulations of an amphiphilic polymer at a hydrophobic/hydrophilic interface

ALINE F. MILLER, MARK R. WILSON*, MELANIE J. COOK and RANDAL W. RICHARDS
Department of Chemistry, University of Durham, South Road, Durham DH1 3LE, UK

(*Received 4 September 2002; accepted 23 October 2002*)

Monte Carlo simulations have been carried out for an off-lattice model of an amphiphilic polymer at a hydrophobic/hydrophilic interface. The model system consists of a polynorbornene backbone with poly(ethylene oxide) (PEO) grafts modelled atomistically at an idealized interface between hydrophobic and hydrophilic regions, which are represented by external potentials. Results are presented for the distribution of PEO chain ends, and the density of PEO segments perpendicular to the surface. The latter is used to provide predictions for neutron reflectivity profiles normal to the surface as a function of the lateral confinement of the PEO grafts. At low surface coverage the simulation results are found to be in good agreement with experimental neutron scattering results from similar polymers studied at the water/air interface.

1. Introduction

The behaviour of a tethered polymer chain is fundamentally different to that of a free polymer chain in solution. In the case where one end of the polymer is bound to the surface, or is confined by a surface layer, the surface places limits on the configurational space available for the chain to explore. For example, for long chains in a good solvent at low surface concentrations (non-interacting chains) a *mushroom regime* is seen, where, close to the surface, solvent swelling of the polymer is limited by the anchoring constraint. At high surface coverage the chains undergo a transition to a *brush regime*. Here, inter-chain steric repulsion, together with the desire for the chains to remain in contact with the solvent, forces the polymer chains to stretch out from the surface to form a layer. The behaviour of such tethered chains has been studied in detail [1] by experiment [2–4] and also by theory [5–8] and simulation [9–11]. The modification of the surface (or interface) properties by the polymer leads to useful applications, including controlling adhesion [12] and stabilizing colloidal dispersions [13]. A general overview of tethered chains is also available in a recent survey of interfacial behaviour of polymers [14].

Amphiphilic polymers with surface active components behave rather differently to an idealized tethered chain. In particular, at low surface coverage, the mushroom regime is not seen. In recent work, Miller *et al.* [15, 16] studied the organization of a well-defined amphiphilic graft copolymer at the air–water interface using neutron reflectivity. Their system consisted of a hydrophobic polynorbornene backbone with hydrophilic poly(ethylene oxide) (PEO) grafts at every monomer unit. The results were consistent with a transition from a *pancake-like* to a *brush-like* arrangement of the hydrophilic grafts as surface concentration, Γ_s, increased. At low surface coverage, the hydrophilic grafts spread out from the backbone forming a layer that was close to the surface of the water [15]. While at high surface concentrations the neutron reflectivity measurements indicated that the chains extended down into the aqueous subphase. Moreover, at the highest values of surface concentration studied [16], the Γ_s dependent thickness of the hydrophilic layer exhibited the scaling law relationship expected for a *brush-like* layer.

The work described here uses Monte Carlo simulations to investigate the polynorbornene–PEO system of reference [15]. A simplified model for the polymer at the interface is described, and the simulation results are used to provide information on the extension of the grafts as a function of lateral confinement. The model is used to supply density distributions for the PEO grafts, which in turn provide predictions for the experimental neutron reflectivity data. The structure of this paper is as follows. The simulation model is described in detail in section 2. Results showing the behaviour of the PEO grafts as a function of lateral confinement (parallel to the surface) are presented in section 3. Finally, we summarize in section 4.

*Author for correspondence. e-mail: mark.wilson@durham.ac.uk

Molecular Physics ISSN 0026–8976 print/ISSN 1362–3028 online © 2003 Taylor & Francis Ltd
http://www.tandf.co.uk/journals
DOI: 10.1080/0026897031000068569

2. Computational

2.1. *Molecular model for an amphiphilic polymer at the air/water interface*

Our computational model is shown schematically in figure 1. It consists of an amphiphilic polymer simulated at a model interface. The polymer studied is modelled atomistically and consists of a hydrophobic backbone composed of norbornene units and hydrophilic grafts composed of poly(ethylene oxide) chains. The model backbone is relatively short (10 units, rather than the 50 units used in [15]) but the grafts themselves are the same length as those used in the neutron reflection work of reference [15]. Rather than explicitly include water molecules in our calculations (which is extremely expensive in terms of computer time) the aqueous phase was represented as a dielectric continuum, and we used a simplified model for an 'air/water' interface which is consistent with experimental data. Firstly, the polymer backbone is excluded from penetrating the surface of the water by a hard-wall potential and secondly, each ethylene oxide (CH_2–CH_2–O) segment moving from the water to the air increases in energy by $a_E = +8.8\,\mathrm{kJ\,mol^{-1}}$. The latter comes from the heat of solution of an ethylene oxide repeat unit in water (5.3–8.8 $\mathrm{kJ\,mol^{-1}}$ [17]). To simulate the influence of surrounding polymer molecules at the surface, the polymer is confined to a cylinder of radius b by a second hard-wall potential. This allows for the mimicking of excluded volume interactions that arise from other molecules at the surface. We note that we cannot simulate effects arising from the inter-penetration of ethylene oxide chains on neighbouring molecules within the framework of this model. The extent to which this occurs in real systems is unknown at this time. Finally, in some simulations, ethylene oxide segments were allowed to interact with a square well potential in the upper part of the 'aqueous' layer. A well of width 3 Å and depth $5\,\mathrm{kJ\,mol^{-1}}$ was used. When explicit solvent molecules are not included, a surface potential well is needed for modelling the surface excess concentration of a surfactant. Since a surface excess is seen experimentally for ungrafted PEO, we expect the surface well to be important in this study.

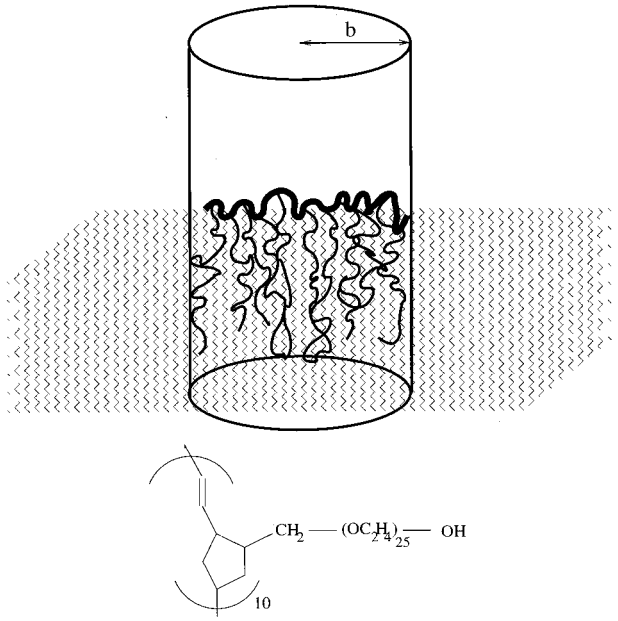

Figure 1. Schematic diagram showing the model system and the structure of the amphiphilic polymer used.

The amphiphilic polymer itself is represented by a series of atomistic potential energy functions

$$E_{\mathrm{total}} = \sum_{\mathrm{angle}} K_\theta(\theta-\theta_0)^2 + \sum_{\mathrm{dihedral}} \left(\sum_{m=1}^{3} \frac{V_m}{2}[1+\cos(m\phi-\delta_m)] \right) + \sum_{i<j} \left(\frac{q_i q_j}{D r_{ij}} + \frac{A_{ij}}{r_{ij}^{12}} - \frac{C_{ij}}{r_{ij}^{6}} \right) f_{ij}, \quad (1)$$

where θ and θ_0 are the actual and reference bond angles, ϕ and δ_m are dihedral and phase angles, and $K_{\theta 1}$ and V_m are force constants representing bond bending and torsional motion respectively. The non-bonded energy between atoms i and j at a distance r_{ij} is represented by a Coulomb plus Lennard-Jones potential, where A_{ij} and C_{ij} can be expressed in terms of the well depth and collision parameters, ε_{ij} and σ_{ij} respectively: $A_{ij} = 4\varepsilon_{ij}\sigma_{ij}^{12}$, $C_{ij} = 4\varepsilon_{ij}\sigma_{ij}^{6}$. As usual, the sum of all non-bonded pairs ($i<j$) in equation (1) excludes all 1–2 and 1–3 bonded interactions. ($f_{ij} = 0.5$ for 1,4 12:6 non-bonded terms, $f_{ij} = 0.125$ for 1,4 electrostatic terms and $f_{ij} = 1$ for all other non-bonded interactions.) In the current work we constrain bonds at their equilibrium values and use the OPLS-AA *all-atom force field* of Jorgensen and co-workers [18–20] for the parameters in equation (1). OPLS-AA treats each atom individually in the simulation, avoiding the problems associated with the *united atom* approximation which tends to be poor for other similar chain systems (e.g. lipid bilayers [21]). The *cis–trans* stereochemistry of the synthesized polymer in [15] is not known. However, from nuclear magnetic resonance measurements the ratio of *trans*/*cis* double bonds is known to be approximately 2:1. In this work we use two separate models for the backbone, one with a *trans* stereochemistry throughout and one with an alternate arrangement of *trans–trans–cis* (*ttc*) double bonds. In both models we explicitly exclude internal rotation about the double bonds. Non-bonded interactions are truncated at 10 Å, and we use a distance dependent dielectric for D in equation (1).

Calculations were carried out for the polymer in the gas phase and for the polymer in the presence of the model interface. In the latter, we used three variants of the model described above: termed *A*, *B*, and *C*. In model *A* we used the *trans* backbone and used no potential well at the 'water surface' to model a system where the chains exhibited no surface excess concentration. In model *B* we used the same backbone as in model *A* but used the 'water surface' potential well (described above), and in model *C* we used the *ttc* backbone with the surface well. A variety of b values were used: ranging from $b = \infty$ Å, corresponding to a free molecule at the interface, to $b = 16$ Å, corresponding to an equivalent surface concentration of $\Gamma_s = 2.5\,\mathrm{mg\,m^{-2}}$ for the polymer in reference [15].

We stress that the model used in this study is relatively primitive. Although individual chains are faithfully represented by the force field, the use of a hard-wall potential (in particular) is a crude representation of the real interactions of surrounding molecules. The advantage of the hard-wall potential is that it is cheap to implement computationally, and can be employed easily to look at the effects of confinement on the behaviour of the graft copolymer. Therefore, the model can be used as a prelude to more sophisticated simulations which use more realistic representations of surrounding molecules and/or represent both the solvent and other polymers explicitly.

2.2. *Monte Carlo simulations*

An initial polymer configuration was generated from gas-phase energy minimization calculations using the program CAChe [22]. This configuration was used as input to the Monte Carlo (MC) calculations. The MC work used the DUMMP program (*D*urham *U*niversity *M*olecular *M*odelling *P*ackage [23]), an internal coordinate MC code written by one of the present authors. All calculations were carried out using Metropolis MC sampling at 300 K. A trial MC move consisted of random changes θ' and ϕ' to a randomly selected angle and dihedral, combined with a random molecular translation $\mathbf{s}'$, and a random molecule rotation using quaternion vectors $\mathbf{q}'$ as described in reference [23]. Maximum values of θ', ϕ', $|\mathbf{s}'|$, and $|\mathbf{q}'|$ were adjusted to obtain acceptance ratios in the range 35–55%. We employed *excluded atom* and Verlet lists to speed up the evaluation of non-bonded interactions, and a link list to speed their compilation. The hard-wall potentials described above allowed unfavourable trial configurations to be quickly eliminated without the need to re-evaluate non-bonded interactions at each MC step. All simulations were carried out at 300 K.

When the radius b of the cylindrical box was large ($\geq$30 Å), it was relatively easy to secure the whole polymer within the hard-wall constraints. This was achieved by applying a distance dependent repulsive potential for atoms at a distance $|\mathbf{r}| > b$ from the centre of the box, and gradually increasing the repulsion until all atoms were within the confines of the cylindrical hard walls. (In this procedure care was required to avoid supplying too much energy too quickly to the polymer chains and thereby producing unphysical conformations with exceptionally high internal energy.) This process was relatively rapid, occurring within approximately 1000 MC steps and was achieved with only minor distortions to the gas-phase equilibrium geometry. Equilibration of the polymer took place within a further period of 10×10^5 trial moves. Figure 2 shows a typical equilibration sequence where the chains are gradually 'captured' by the 'aqueous' phase. For $21 < b < 30$ Å this process was still relatively rapid and in each case required less than 2×10^5 MC moves. Production runs were then carried out over a further period of 25×10^5 trial moves. However, for systems with $b \leq 21$ Å, the above procedure had to be modified drastically. For these systems, several million trial moves were required to confine the polymer inside the hard-wall constraints. (Here, we concentrated on first confining the backbone in the box and then subsequently working with the PEO chains.) We then applied a distance dependent potential to speed up the capture of the PEO chains by the aqueous phase during a further 7.5×10^5 trial moves. Finally, longer equilibration runs (60×10^5 trial moves) and production runs (60×10^5 trial moves) were required to obtain results.

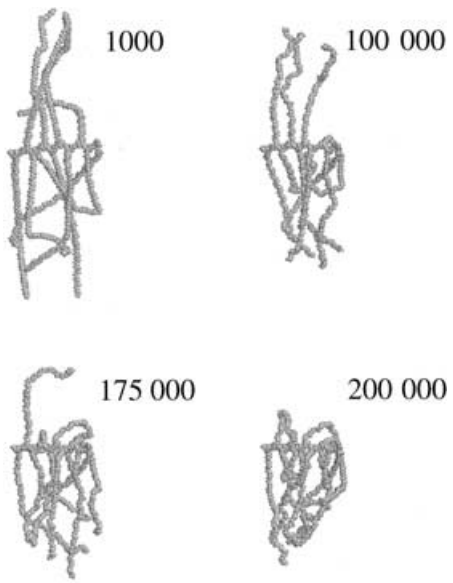

Figure 2. Snapshots from the equilibration run of the $b = 30$ Å system, showing the 'capture' of the PEO grafts by the 'aqueous' phase. Snapshots are taken after 1000, 100 000, 175 000, and 200 000 MC steps.

3. Results and discussion

Simulation results were obtained for the following data: model *A*, $b = \infty$, 75, 55, 50, 40, 30 Å; model *B*, $b = \infty$, 55, 40, 30 Å; model *C*, $b = \infty$, 55, 40, 30, 20, 18, 16 Å. In figure 3 we show a typical 'density' profile obtained, in this case, for model *A* at $b = 50$ Å, plotted as the mean mass per unit distance normal to the surface, $\langle \rho' \rangle$.† As expected the polynorbornene backbone is seen as a sharp peak situated at the interface. The shape of this peak remains fairly constant for the majority of simulations. However, for values of $b < 30$ Å there is evidence for tilting of the backbone and this leads to a slight broadening of this peak. The PEO grafts extend down from the interface into the 'aqueous' subphase forming a *brush-like* structure. This is expected for this value of *b*, which corresponds to a relatively high surface concentration of $0.7\,\mathrm{mg\,m^{-2}}$ where molecules are no longer isolated but are constrained by their neighbours. There is a small peak in the PEO density profile at positive distances (i.e. above the interface). This occurs because of the constraints imposed by the relatively rigid polymer backbone, such that all the grafts are unable to point directly downwards into the aqueous phase at the same time, and must 'loop over' in order to contact the water, as seen in the equilibration snapshots of figure 2. This effect is largest for confined geometries, at low *b* values, where the hard-wall constraints impose strict lateral confinement on the positions of both the backbone and the grafts. This can only be accommodated by small distortions in the backbone (resulting in it no longer lying flat on the surface of the water), and by the grafts sticking out further into the air before looping back into the subphase. Monitoring the instantaneous position of individual chains during the course of the simulation, indicates that there is considerable movement of individual PEO segments into and out of the water during the course of the simulations. Consequently, even at low *b* values, the system remains in constant motion, with individual chains free to move up and down relative to the interface.

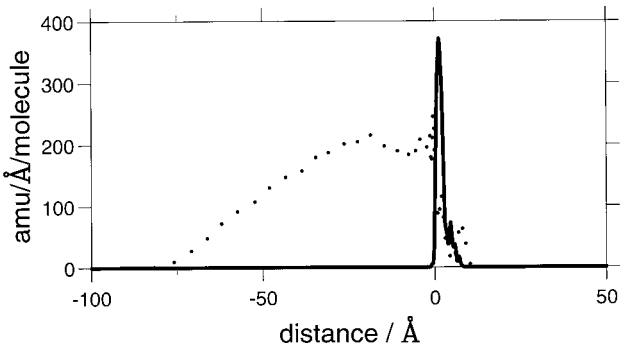

Figure 3. 'Density' distribution functions for the mean mass per unit distance perpendicular to the surface for model *A* at $b = 50$ Å. Bold curve, backbone; dotted curve, PEO grafts. The interface is situated at zero, with negative distances corresponding to the aqueous subphase.

†Plotting the mass distribution in this way aids comparison with different *b* values as the area under the curve is independent of *b*.

The overall shape of the PEO 'density' profile in figure 3 is of some interest. The PEO density rises from a value close to zero at the interface and then decays to zero. The initial decay is parabolic, but there is an extended tail. Kent *et al.* [3] have carried out neutron reflectivity studies of Langmuir monolayers of polydimethylsiloxane–polystyrene (PDMS-b-PS) diblock copolymers spread on ethyl benzoate (EB), which acts as a good solvent for polystyrene. The fitted density profiles are consistent with a smooth rise from almost zero at the surface to a maximum, followed by a parabolic decay, with an extended tail. Such a profile also arises from numerical solutions to the self-consistent field (SCF) equations of Baranowski and Whitmore [8, 24] in good and Θ solvents. While the simulated profiles for model *A* exhibit the same decay as this experiment, we see no strong evidence for a depletion layer close to the surface. This is caused by the relative shortness of the PEO chains in this study (only 25 monomers).

There is a significant transformation in the polymer microstructure resulting from changes to the boundary condition *b*. To show this we plot $\langle \rho' \rangle$ for each model at three separate *b* values in figure 4, and plot the distribution function for the terminal oxygen of the grafts in figure 5. The potential well has a dramatic effect on the positional ordering of PEO chains. At high values of *b* the behaviour of the PEO grafts for model *A* contrasts strongly with their behaviour for models *B* and *C*. In models *B* and *C* the peak in $\langle \rho' \rangle$ close to the interface indicates that the PEO chains stretch out from the backbone to occupy the surface region for high *b* values, but undergo a transition to a more *brush-like* regime at higher surface coverage (low values of *b*). However, even for $b = 30$ Å the surface peak is still visible in figure 4, indicating that the surface continues to have an effect on the polymer microstructure. The differences in behaviour for models *B* and *C* are rather small for *b* values down to 30 Å. However, below $b = 30$ Å we were unable to achieve equilibration for *all-trans* backbones. This is indicative of the greater conformational freedom of the PEO chains when *cis* linkages are included in the polynorbornene. However, in the experiment the effects of this are likely to be manifested only at high surface concentrations.

The form of the terminal oxygen distribution function suggests that chains 'curl up' to a considerable degree, and do not remain in their most extended conformations. In model *A*, there is a small probability for the end

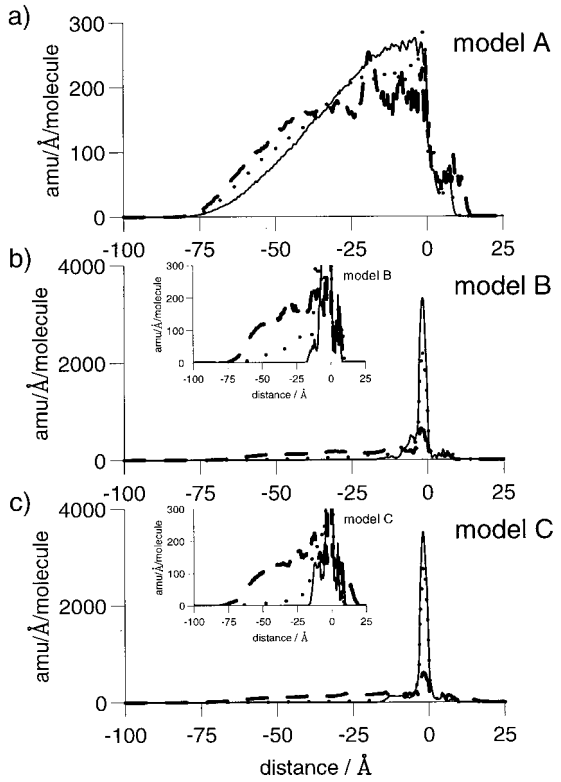

Figure 4. 'Density' distribution functions for the mean mass per unit distance perpendicular to the surface for PEO grafts. Bold curve, $b = \infty$ Å; dotted curve, $b = 55$ Å; dashed curve, $b = 30$ Å.

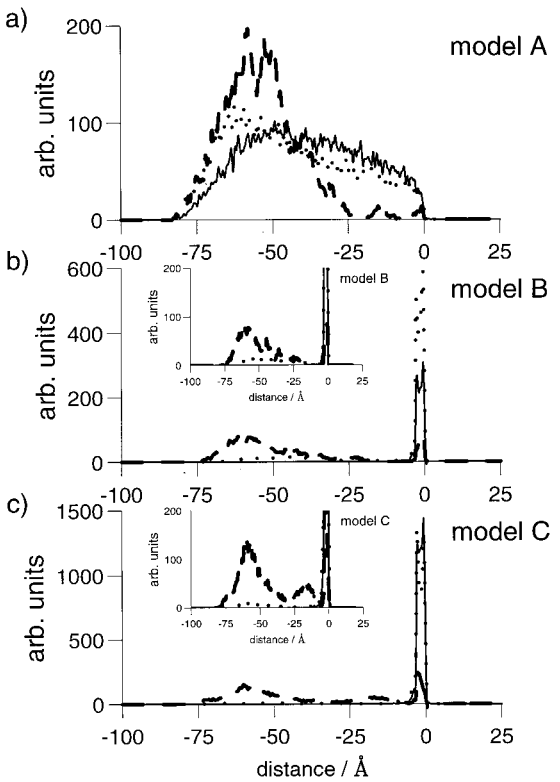

Figure 5. Distribution functions for the terminal oxygen in the PEO grafts for models *A*, *B* and *C*. Bold curve, $b = \infty$ Å; dotted curve, $b = 55$ Å; dashed curve, $b = 30$ Å.

of the chain to be close to the surface for each b value. The maximum in the curve shifts further from the surface as b is reduced and consequently the terminal oxygens are forced to extend deeper into the subphase. Lai and Binder [10] show similar curves for Monte Carlo simulations of a bond fluctuation model of tethered chains and also find a non-zero probability for the chain ends being at the surface. This result is not in agreement with the SCF theory of reference [7], but can be attributed to the relatively short chain lengths used in the simulations.

For models *B* and *C*, the terminal oxygens remain close to the surface for high b values, but for $b = 30$ Å we see evidence for a distribution function composed of two separate elements: a peak in the same position as model *A*, in addition to the sharp peak at the interface. This is consistent with some chains remaining at the surface, while others are forced down into the subphase. Observations of Monte Carlo snapshot configurations compiled into movies confirm this by showing that, during the course of a simulation, chains are continually escaping from and being captured by the surface potential well. This behaviour is fundamentally different to that exhibited in a normal transition to *brush-like* behaviour.

To compare the computed density profiles with the experimental data of reference [15], the ethylene oxide volume fraction ϕ_{EO} was calculated for unit layers normal to the surface and multiplied by the scattering length density for a deuterated ethylene oxide monomer ($\rho_{EO} = 6.33 \times 10^{-6}$ Å^{-2}) to obtain a scattering length density ρ for each unit layer. The simulated reflectivity profile was then calculated from ρ using an optical matrix technique [25]. In figure 6 we show the results for models *A*, *B* and *C* for a value of $b = 55$ Å, which corresponds to the lowest surface concentration $\Gamma_s = 0.3\,\text{mg}\,\text{m}^{-2}$ at which scattering could be detected for the experimental systems. The simulated reflectivity profile for model *A* is poor, and fails to reproduce the slope of the experimental data. The results from models *B* and *C* are rather better and reproduce the general shape and slope of the curve, with the *ttc* configuration for the polymer giving the best fit to the experimental data. At this low surface coverage molecules are almost isolated on the surface. However, a comparison of the density profiles for $b = 55$ Å and $b = \infty$ Å indicates a slight shift in the chain distribution towards the surface for the latter. This occurs because the removal of the

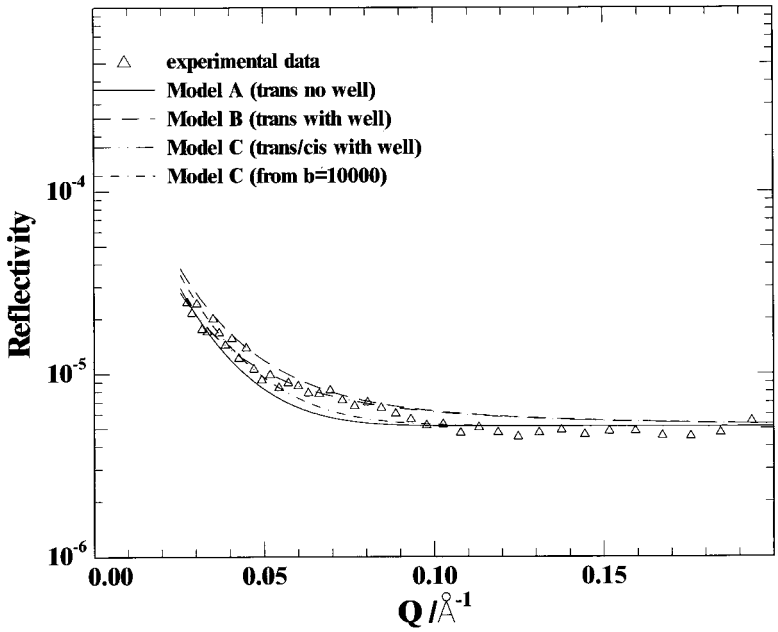

Figure 6. Simulated and experimental neutron reflectivity data for a surface concentration of $0.3\,\mathrm{mg\,m^{-2}}$.

hard cylinder constraint allows the chains to *stretch* slightly so that more of the chain can lie at the interface. Use of the $b = \infty$ Å profile for model *C* in figure 6 improves the agreement with experiment further. Consequently, it seems that the correct interpretation of the experimental data is as follows. At $\Gamma_s = 0.3\,\mathrm{mg\,m^{-2}}$, the ethylene oxide grafts stretch out from the polymer backbone to lie almost completely at the interface (as shown in figure 7), and the small degree of inter-penetration of grafts from neighbouring molecules that must occur for this surface coverage (the overlap concentration is $0.11\,\mathrm{mg\,m^{-2}}$) has no significant effect on the density profile of the grafts normal to the surface.

In reference [15], the optical matrix method has been used to provide a fit to the neutron reflectivity data by assuming a uniform PEO layer close to the surface, plus a parabolic decay. A comparison of volume fractions from the optical matrix method fit and from model *C* at $b = 55$ Å is given in figure 8. Two main differences are apparent: the tail in ϕ_{EO} for the simulation data extends to a distance of at least 20 Å from the surface, and (in contrast to the experimental fit) a small amount of PEO remains above the surface for the simulated data. The latter would not give rise to a strong signal in the experiment. However, we are able to test the simulation predictions that some PEO lies above the surface by calculating the total amount of PEO in the subphase accounted for in the experimental fits. Unfortunately, the latter varies somewhat according to the precise functional form chosen for the fitting. In most fits, between 95–100% is accounted for in the subphase; and

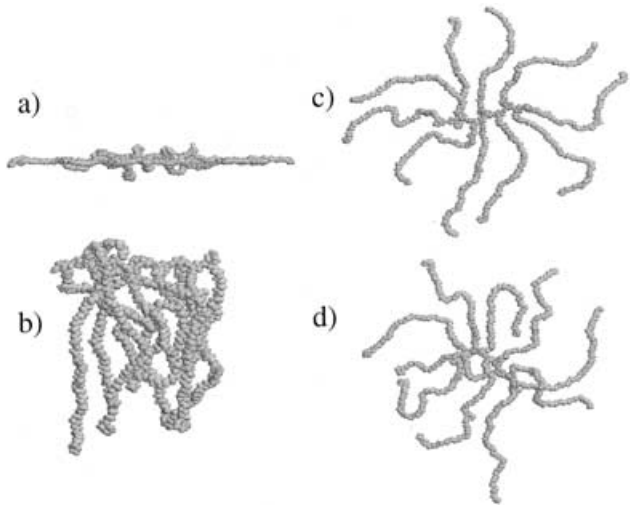

Figure 7. Snapshots showing the changing structure of the polymer for (*a*) all-*trans* backbone $b = \infty$ Å, (*b*) all-*trans* backbone $b = 30$ Å, (*c*) all-*trans* backbone $b = \infty$ Å (viewed from above), (*d*) *ttc* backbone $b = \infty$ Å (viewed from above).

for this low surface concentration a uniform layer plus parabola fit can account for essentially all PEO. For comparison, in table 1 we have calculated the percentage of the ethylene oxide groups that remain above the surface for model *C*, together with the fraction greater than 2 Å above the interface. As *b* is reduced the results indicate that more PEO is forced above the surface, because of the need for some chains to 'loop over' within a confined geometry as shown in figure 2.

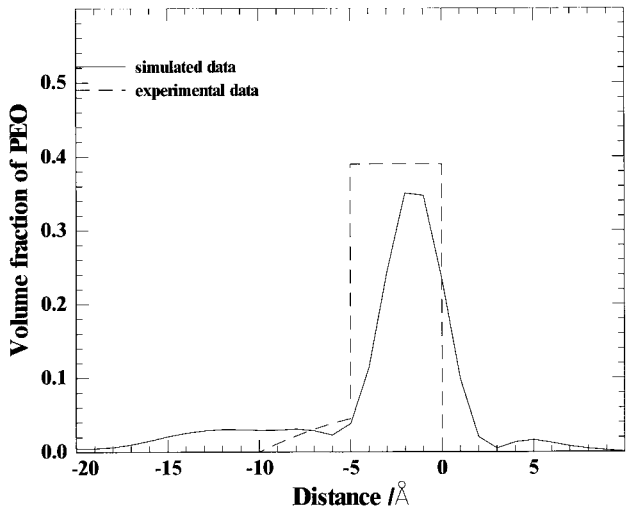

Figure 8. Simulated ($b = 55$ Å) and experimental (from fit) volume fraction data for a surface concentration of $0.3\,\mathrm{mg\,m^{-2}}$.

Table 1. Percentage of ethylene oxide density above the interface (> 0 Å), and greater than 2 Å above the interface for model *C*.

b/Å	% > 0 Å	% > 2 Å
∞	9.2	2.9
55	9.4	3.2
40	11.4	7.2
30	12.5	9.3
21	29.3	27.0
16	30.9	27.6

At the lowest two b values, the polymer backbone is forced to tilt and this leads to a larger percentage ($\approx$ 30%) of the PEO lying above the surface. In the experiment this would only happen for extremely high surface concentrations where crowding of molecules would force the backbone to tilt in order to provide enough space for the PEO grafts. Consequently, while the low density results are consistent with experiment, the higher density results appear not to be. This is confirmed in figure 9 by using the simulations to calculate the neutron reflectivity profiles for higher equivalent surface concentrations of model *C*. For lower b values the simulation is no longer able to reproduce the reflectivity curves. The failure can be accounted for by an overprediction of the amount of PEO above the interface and an exaggeration of the amount of PEO deep in the subphase. Both of these deficiencies are due to the rigidity of the hard-wall constraints.

The tail in ϕ_{EO} of figure 8 has not been allowed for in the fit to experimental data, but the presence of this (for the low volume fractions shown in the simulation) makes little difference to the reflectivity curve, so this

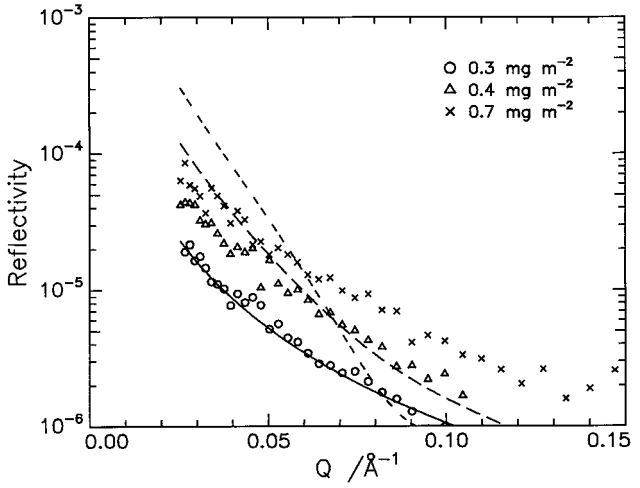

Figure 9. Simulated (model *C*) and experimental neutron reflectivity data for three surface concentrations: solid curve, $0.3\,\mathrm{mg\,m^{-2}}$; long dashed curve, $0.4\,\mathrm{mg\,m^{-2}}$; short dashed curve, $0.7\,\mathrm{mg\,m^{-2}}$.

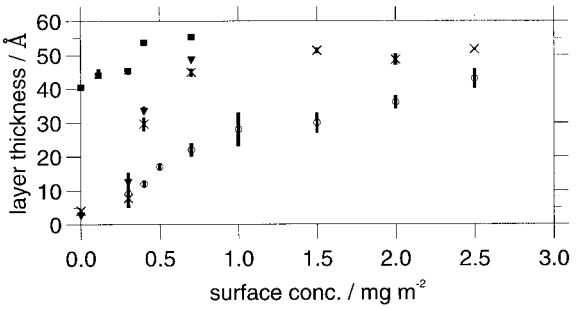

Figure 10. Layer thickness as a function of surface concentration. Open circles, experimental data (from fit); filled squares, model *A*; filled triangles, model *B*; crosses, model *C*.

prediction is difficult to test experimentally. However (as discussed above), such a tail is consistent with the neutron reflectivity data of Kent and co-workers for PDMS-b-PS copolymers. So it seems likely that the simulation is pointing to a real feature of the graft density profile.

Finally, it is interesting to compare the experimental and calculated layer thicknesses for the polymer. In figure 10 we plot the mean length of the chain perpendicular to the surface $\langle r_z \rangle$ for models *A*–*C* and compare the data with the polymer thickness obtained from fitting a uniform plus parabolic decay to the experimental reflectivity curves. Model *A* clearly overestimates the layer thickness at all surface coverages. Models *B* and *C* are closer to the experimental data. However, as surface coverage increases, these data also overestimate the thickness of the layer. Undoubtedly this is caused by the fact that the rigid hard-wall constraints provide less space for the PEO chains than would be the case if the molecule was surrounded by

flexible neighbours, which would allow the interpenetration of the PEO chains into a region of space occupied by adjacent molecules. We note the change in slope of the experimental curve in figure 10. This is echoed in the simulation data, which show also a change in the slope of the layer thickness curve at approximately $0.7\,\mathrm{mg\,m^{-2}}$($b = 30$ Å). Theory predicts that the layer thickness should scale as $\sigma^{1/3}N$ and this trend is seen also in Monte Carlo lattice simulations of the bond fluctuation model [10]. Between 0.3–$1.0\,\mathrm{mg\,m^{-2}}$ the experimental exponent for σ is 0.77, but recent work by Miller [16], for higher surface coverages, suggests that the exponent changes to 0.33 for surface concentrations in excess of $1.5\,\mathrm{mg\,m^{-2}}$. In the current study, computational expense limits the number of simulations at low b and we have been unable to test this prediction. However, the qualitative information from the simulations (as discussed above) points to the fact that it is only when the surface coverage gets sufficiently high to stop all chains occupying the surface, that true *brush-like* behaviour can arise.

4. Conclusions

We have simulated a simple atomistic model for an amphiphilic polymer composed of a polynorbornene backbone with PEO grafts at a model interface. Three variants of the model were used. In each case the polymer was confined to a cylinder of radius b to model the lateral constraints imposed by other molecules, and in two variants of the model the PEO grafts were able to interact with a surface potential well. Without the surface well the PEO chains behaved like polymer brushes, but exhibited no noticeable depletion layer close to the surface because of the relative shortness of the PEO chains (25 monomers). With the surface well the chains exhibited a transition from a molecular arrangement, which had the PEO chains close to the interface at high values of b, to a brush-like regime with the chains stretching out normal to the interface at low b values (equivalent to high surface coverage). At low surface concentrations we were able to model successfully experimental neutron reflectivity profiles obtained for the same polymer. However, at higher surface concentrations the simulations overpredict the thickness of the PEO layers. Here the hard-wall constraints used provide too severe a constraint in comparison to neighbouring molecules.

The good qualitative understanding provided by the simple models employed in this study, has prompted us to look at the behaviour of this polymer at a 'realistic interface' provided by explicit water molecules. These calculations are currently under way in our laboratory. Such studies are extremely expensive in terms of computer time, but promise to yield further insights into the behaviour of these interesting polymers at the water–air interface.

The authors wish to thank the University of Durham IT service for providing computer time on its parallel Silicon Graphics system, and the UK Engineering and Physical Sciences Research Council (EPSRC) for providing computer time on a Cray T3E. AFM and MJC wish to thank the EPSRC for providing research studentships (1997–2000).

References

[1] Szleifer, I., and Carignano, M. A., 1996, *Adv. Chem. Phys.*, **94,** 165, provides a review.
[2] Kent, M. S., Lee, L. T., Farnoux, B., and Rondelez, F., 1992, *Macromolecules*, **25,** 6240.
[3] Kent, M. S., Lee, L. T., Factor, B. J., Rondelez, F., and Smith, G. S., 1995, *J. chem. Phys.*, **103,** 2320.
[4] Kent, M. S., Majewski, J., Smith, G. S., Lee, L. T., and Satija, S., 1998, *J. chem. Phys.*, **108,** 5635.
[5] Alexander, S., 1977, *J. Phys. (France)*, **38,** 983.
[6] de Gennes, P. G., 1980, *Macromolecules*, **13,** 1069.
[7] Milner, S. T., Witten, T. A., and Cates, M. E., 1988, *Macromolecules*, **21,** 2610.
[8] Baranowski, R., and Whitmore, M. D., 1998, *J. chem. Phys.*, **108,** 9885.
[9] Chakrabarti, A., and Toral, R., 1990, *Macromolecules*, **23,** 2016.
[10] Lai, P.-Y., and Binder, K., 1991, *J. chem. Phys.*, **95,** 9288.
[11] Lai, P.-Y., and Binder, K., 1992, *J. chem. Phys.*, **97,** 586.
[12] Lèger, L., Raphael, E., and Hervet, H., 1999, *Adv. Poly. Sci.*, **138,** 185.
[13] Napper, D. H., 1983, *Polymeric Stabilization of Colloidal Dispersions* (New York: Academic Press).
[14] Jones, R. A. L., and Richards, R. W., 1999, *Polymers at Surfaces and Interfaces* (Cambridge: Cambridge University Press).
[15] Miller, A. F., Richards, R. W., and Webster, J. R. P., 2000, *Macromolecules*, **33,** 7618.
[16] Miller, A. F., 2000, PhD thesis, University of Durham.
[17] Orwoll, R. A., 1999, *Polymer Handbook*, 4th edition, edited by J. Brandrup, E. H. Immergut and E. A. Gralke (New York: Wiley).
[18] Jorgensen, W. L., Maxwell, D. S., and Tirado-Rives, J., 1996, *J. Am. chem. Soc.*, **118,** 11 225.
[19] Jorgensen, W. L., Maxwell, D. S., and Tirado-Rives, J., 1996, *J. Am. chem. Soc.*, **118,** 11 225, *support material.*
[20] Jorgensen, W. L., and Nguyen, T. B., 1993, *J. comput. Chem.*, **14,** 195.
[21] Tobias, D. J., Tu, K., and Klein, M. L., 1997, *Curr. Opin. Colloid & Interface Sci.*, **2,** 15.
[22] *CAChe Satellite: A Chemists Guide to CAChe for Windows*, 1995, Oxford Molecular Group Inc.
[23] Wilson, M. R., 1996, *Liq. Cryst.*, **21,** 437.
[24] Baranowski, R., and Whitmore, M. D., 1995, *J. chem. Phys.*, **103,** 2343.
[25] Heavens, O. S., 1995, *Optical Properties of Thin Films* (London: Butterworths).